

Refereed Proceedings

*The 12th International Conference on
Fluidization - New Horizons in Fluidization
Engineering*

Engineering Conferences International

Year 2007

Modeling Mercury Capture by Powdered
Activated Carbon in a Fluidized Bed
Reactor

Fabrizio Scala*

Riccardo Chirone[†]

Amedeo Lancia[‡]

*CNR, Italy, scala@irc.cnr.it

[†]CNR, Italy, chirone@irc.na.cnr.it

[‡]Università degli Studi di Napoli Federico II

This paper is posted at ECI Digital Archives.

http://dc.engconfintl.org/fluidization_xii/72

Scala et al.: Modelling Mercury Capture by Powdered Activated Carbon

MODELING MERCURY CAPTURE BY POWDERED ACTIVATED CARBON IN A FLUIDIZED BED REACTOR

Fabrizio Scala¹, Riccardo Chirone¹, Amedeo Lancia²

1 - Istituto di Ricerche sulla Combustione – CNR

2 - Dipartimento di Ingegneria Chimica – Università degli Studi di Napoli Federico II

Piazzale Tecchio 80, 80125 – Napoli (Italy)

T: +39-081-768-2969; F: +39-081-593-6936; E: scala@irc.cnr.it

ABSTRACT

A steady state model of mercury capture on activated carbon in a bubbling fluidized bed of inert material is presented. The model takes into account the fluidized bed fluid-dynamics, the presence of both free and adhered carbon in the reactor as well as mass transfer limitations and mercury adsorption equilibrium. The activated carbon adsorption parameters and the relative amount of free versus adhered carbon in the reactor have been estimated with purposely designed experiments. Model results are compared with results from mercury capture experiments conducted with commercial powdered activated carbon at 100°C in a lab-scale pyrex fluidized bed of inert particles. The role of free versus adhered carbon in determining the overall mercury capture efficiency is discussed.

INTRODUCTION

Mercury compounds have been recognized as persistent, bioaccumulative and toxic pollutants, extremely dangerous for the ecosystem and for human health (1,2). Gaseous emissions into the atmosphere from anthropogenic sources (mainly coal combustors and waste incinerators) are emitted in the form of elemental (Hg^0) and oxidized mercury (Hg^{2+}), the second being simpler to control due to its high reactivity and solubility in water. Unlike waste incinerators, which emit high concentrations of mercury mostly in the oxidized form, coal-fired power plants emit very dilute concentrations of both Hg^0 and Hg^{2+} , whose proportions can vary widely. In the last decade industrialized countries have been setting progressively tighter limits for mercury emissions from waste incinerators. Due to increasing concern for mercury emissions from coal-fired power plants, stringent limits are under consideration in many countries also for these facilities.

Mercury removal from combustion/incineration flue gas is typically accomplished with the use of activated carbon as an adsorbent (3,4). The most economically attractive contact design is the direct in-duct injection of powdered carbon, with the subsequent collection in a fabric filter (FF) or in an electrostatic precipitator (ESP). However, this design provides a very short contact time (few seconds) between the flue gas and the adsorbent in the ductwork. When the particulate matter control device is an ESP (as in most of the existing utility boilers) this results in a low carbon utilization.

The use of a bubbling fluidized bed of inert material, upstream of a particulate matter control device, to increase the utilization of activated carbon in the flue gas ducts has been recently proposed (5). The starting point was the experimental observation that a bubbling fluidized bed of coarse granular material may act as a filter capable of increasing both the residence time and the specific gas-solid contact surface of a powder carried by a gas stream (6).

Mercury capture experiments carried out at 100°C in a lab-scale pyrex reactor were reported (5). Powdered activated carbon was continuously injected in the reactor and both mercury concentration and carbon elutriation rate were followed at the outlet. Results showed that the presence of a fluidized bed of inert material led to an increase of mercury capture efficiency with respect to an entrained bed configuration. This was explained by the larger activated carbon loading and gas-solid contact time that establishes in the reaction zone, because of the increased surface area available for activated carbon adhesion in the fluidized bed.

In this paper a steady state 1-D model of mercury capture on activated carbon in a fluidized bed is presented, taking into account the fluidized bed fluid-dynamics, the presence of both free and adhered carbon in the bed as well as mass transfer limitations and mercury adsorption equilibrium. Model results have been compared with results from available mercury capture experiments, to discriminate between the controlling phenomena of the process.

MODEL DESCRIPTION

The model is based on the following simplifying assumptions: 1) Mercury exists only as Hg^0 in the gas (this provides a conservative measure of total Hg^0+Hg^{2+} removal). 2) Mercury adsorption does not depend on the presence of gas species other than Hg^0 . 3) Adsorbent and inert particles are both spherical and uniform in size. 4) The inert particles keep their initial size and are large enough not to be elutriated from the bed. 5) Both the gas and the activated carbon flow rates are constant. 6) The temperature is constant and uniform through the bed. 7) Mercury adsorption on the activated carbon particles is based on equilibrium conditions between the gas and the adsorbed phase. Radial gradients of mercury inside the particles are neglected.

Fluidized bed fluid-dynamics

The bed is modeled following the two phase fluidization approach, assuming both gas and solids in the dense phase well mixed, and gas in the bubble phase in plug flow. An average bubble size is assumed and calculated according to Darton et al. (7). The bubble-emulsion mass transfer coefficient is calculated according to Sit & Grace (8).

The activated carbon particles are injected in the reactor from the bottom section and enter both the emulsion phase and the bubble phase. The activated carbon exits from the reactor with the flue gas by elutriation. At the steady state the inlet and the outlet carbon flow rates must be equal. In these conditions there is no accumulation in the reactor, where a steady carbon loading establishes. In the emulsion phase the activated carbon dispersed in the gas interacts with the inert particles and adheres on their surface by Van der Waals and/or electrostatic forces. On the other hand, the activated carbon adhered on the inert particles' surface can be removed by attrition.

In principle the total carbon loading within the reactor can be divided into two

contributions: a free carbon loading consisting in the activated carbon transported with the gas stream (both in the emulsion and in the bubble phase), and an adhered carbon loading consisting in the activated carbon attached on the fluidized bed inert particles. It is obvious that the free and the adhered carbon loadings are characterized by a short and a long residence time within the reactor, respectively.

Material balances

The process of mercury vapor adsorption on the activated carbon is schematized as a series of two steps: 1) Mass transfer from the bulk gas to the external surface of the carbon particle through the gas boundary layer. 2) Surface adsorption on the particle.

In the dense phase mercury is adsorbed on the carbon adhered on the inert bed and on the free carbon in the gas. The material balance on mercury can be written as:

$$U_{mf} \cdot A \cdot (c_0 - c_d) - k_g^{free} \cdot S_{free}^d \cdot (c_d - c_{eq}^{free,d}) - k_g^{ad} \cdot S_{ad} \cdot (c_d - c_{eq}^{ad}) + Q_b = 0 \quad (1)$$

where the mercury exchange between the gas in bubble and emulsion phases is:

$$Q_b = A \cdot \frac{(U - U_{mf})}{U_b} \cdot K_{be} \cdot \int_0^h [c_b(z) - c_d] \cdot dz \quad (2)$$

In the bubble phase mercury is adsorbed on the free carbon in the gas along the bed height. The differential material balance on mercury can be written as:

$$\begin{cases} -U_b \cdot \frac{dc_b(z)}{dz} = K_{be} \cdot [c_b(z) - c_d] + k_g^{free} \cdot [c_b(z) - c_{eq}^{free,b}] \cdot \frac{S_{free}^b}{V_b} \\ c_b(0) = c_0 \end{cases} \quad (3)$$

The outlet mercury concentration is simply given by:

$$c_{out} = \frac{c_d \cdot U_{mf} + c_b(h) \cdot (U - U_{mf})}{U} \quad (4)$$

Following the Langmuir theory, in each phase the equilibrium gas mercury concentration (c_{eq}) can be related to the mercury uptake on the adsorbent (ω_{eq}) by:

$$c_{eq} = \frac{1}{K_{eq}} \left(\frac{\omega_{eq} / \omega_{max}}{1 - \omega_{eq} / \omega_{max}} \right) \quad (5)$$

Parameters estimation

The mass transfer coefficient for the free activated carbon particles in both the dense phase and bubble phase can be calculated as:

$$k_g^{free} = \frac{Sh^{free} \cdot D_{Hg}}{d_{ac}} = \frac{2 \cdot D_{Hg}}{d_{ac}} \quad (6)$$

where it has been considered that the Sherwood number is equal to the limiting theoretical value of 2. This is supported by the fact that for very small particle size the slip velocity between the carbon particles and the gas is expected to be negligible.

For the activated carbon adhered on the inert particles' surface, the relevant length scale for the diffusion process is the inert particle diameter. In this case:

$$k_g^{ad} = \frac{Sh^{ad} \cdot D_{Hg}}{d_{in}} \quad (7)$$

where:

$$Sh^{ad} = 2 \cdot \varepsilon_{mf} + 0.69 \cdot \left[\frac{\rho_{gas} \cdot (U_{mf} / \varepsilon_{mf}) \cdot d_{in}}{\mu_{gas}} \right]^{1/2} \cdot \left(\frac{\mu_{gas}}{\rho_{gas} \cdot D_{Hg}} \right)^{1/3} \quad (8)$$

Molecular diffusivity of elemental mercury in the gas at 100°C was estimated to be $D_{Hg} = 0.2 \times 10^{-4} \text{ m}^2/\text{s}$.

The activated carbon exposed surface in each phase has been estimated on the basis of the two following assumptions: 1) The exposed surface for the activated carbon adhered on the inert bed is equal to the bed particles surface multiplied for a surface coverage factor (σ). 2) The activated carbon concentration in the gas is equal in the bubble phase and in the interstitial gas of the dense phase. The adhered and free carbon exposed surfaces are given by:

$$\begin{cases} S_{ad} = \frac{S_{in} \cdot m_{in}}{V_{in} \cdot \rho_{in}} \cdot \sigma \\ S_{free} = S_{free}^b + S_{free}^d = \frac{S_{ac} \cdot m_{ac}^{free}}{V_{ac} \cdot \rho_{ac}} \end{cases} \quad (9)$$

The relative proportion between the free carbon exposed surfaces in the dense and bubble phases is simply given by:

$$S_{free}^d = S_{free}^b \cdot \frac{\delta}{\varepsilon_{mf} \cdot (1 - \delta)} \quad (10)$$

where the volumetric fraction of the bubbles in the bed is:

$$\delta = \frac{(U - U_{mf})}{U_b} \quad (11)$$

The mass of activated carbon adhered on the inert bed can be estimated by assuming that the carbon particles adhere on the bed particles' surface as a spherical shell (monolayer), with a thickness equal to the carbon particle diameter and a packing factor ≈ 0.6 , and considering the surface coverage factor:

$$m_{ac}^{ad} = \left(\frac{m_{in}}{V_{in} \cdot \rho_{in}} \right) \cdot (\rho_{ac} \cdot V_{shell} \cdot 0.6) \cdot \sigma \quad (12)$$

RESULTS

Results from the model described in the previous section have been compared with results from elemental mercury capture experiments conducted in a lab-scale pyrex fluidized bed, 65 mm ID (5). The experiments were carried out at 100°C and the Hg^0 inlet concentration was 90–95 $\mu\text{g}/\text{m}^3$. The bed consisted in 300 g of quartz particles (212–400 μm , $U_{mf} = 0.05 \text{ m/s}$), corresponding to an unexpanded bed height of 6.5 cm. The total superficial gas velocity in the column was fixed at either 0.15 or 0.32 m/s, corresponding to bubbling conditions. No slugging was observed in the tests. The activated carbon feed rate was varied in the range 5–8 g/h. A widely used commercial powdered activated carbon (Darco FGD – lignite derived) was used in the tests. The carbon powder had a Sauter mean diameter of 8.2 μm .

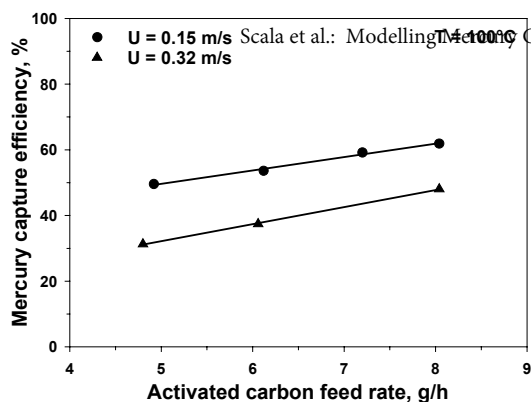


Figure 1: Experimental steady state Hg^0 capture efficiency as a function of the activated carbon feed rate (5).

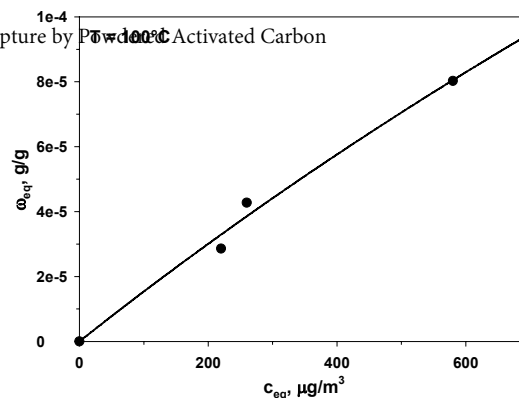


Figure 2: Langmuir adsorption isotherm for Hg^0 on Darco FGD activated carbon at $T = 100^\circ\text{C}$.

Figure 1 reports the experimental steady state mercury capture efficiency (defined as: $(c_0 - c_{out})/c_0 \times 100$) as a function of the activated carbon feed rate in tests carried out in the fluidized bed, at the two gas superficial velocities. The analysis of the data reveals the following trends: a) the Hg^0 capture efficiency increases with the activated carbon feed rate; b) the Hg^0 capture efficiency increases when the gas superficial velocity decreases. These two trends are easily explained if one considers that by increasing the activated carbon feed rate (at the same gas velocity) or by decreasing the gas superficial velocity (at the same carbon feed rate) the carbon-to-mercury ratio inside the reactor increases.

The activated carbon adsorption capacity was separately characterized in a fixed bed apparatus under conditions similar to the fluidized bed experiments. Details of the fixed bed apparatus and experimental procedures are reported elsewhere (9).

Breakthrough curves were obtained by mercury adsorption batch experiments in a fixed bed of 0.2 g activated carbon at 100°C with a gas flow rate of $0.21 \text{ m}^3/\text{h}$ and mercury inlet concentration in the range $220\text{--}580 \mu\text{g}/\text{m}^3$. Figure 2 reports the Langmuir isotherm at 100°C obtained by fitting the experimental capacity data with eq. 5. It is noted that at the mercury gas concentrations used in the fluidized bed experiments, the Langmuir isotherm is approximately linear. To find the maximum equilibrium mercury concentration relevant to the fluidized bed experiments, the maximum uptake of mercury in the activated carbon must be estimated. Using an average particle residence time in the bed of 2-4 s (whose estimation will be detailed later on), and assuming external diffusion control for the mercury capture process (the maximum possible rate), it can be shown that the mercury uptake on the activated carbon is so low that the corresponding equilibrium gas concentration is some orders of magnitude lower than the gas bulk concentration (4). For this reason it was put $c_{eq} \approx 0$ in eqs 1 and 3.

Model calculations were carried out by setting the values of the operating variables equal to those used in the fluidized bed experiments. With the parameters estimated as detailed in the previous section, the model can be used to predict the outlet gas mercury concentration (i.e. the mercury capture efficiency), once the free and adhered activated carbon masses in the bed are given.

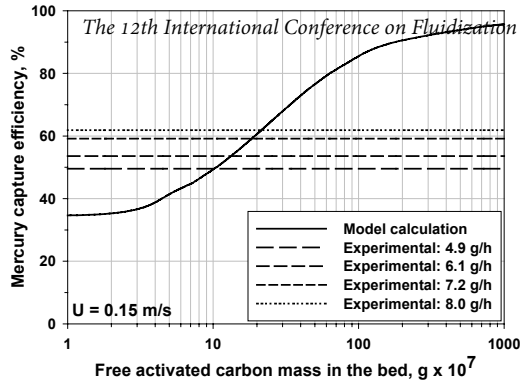


Figure 3: Calculated steady state Hg^0 capture efficiency as a function of the free activated carbon mass in the bed. $U = 0.15$ m/s.

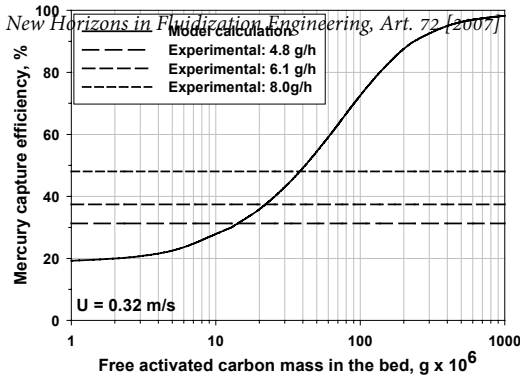


Figure 4: Calculated steady state Hg^0 capture efficiency as a function of the free activated carbon mass in the bed. $U = 0.32$ m/s.

The adhered activated carbon mass in the bed was estimated from the experimental data reported in Fig. 1 using the following procedure. If we extrapolate the experimental data reported in Fig. 1 at zero activated carbon feed rate, the Hg^0 capture efficiency relative to the sole adhered carbon contribution is obtained. This is equal to set $m_{ac}^{free} = 0$. With this condition, and using the mercury capture efficiency values extrapolated at zero carbon feed rate, the model can be solved with the only unknown variable m_{ac}^{ad} . Interestingly, by using this procedure for the two fluidization velocities (0.15 and 0.32 m/s), the same value of adhered activated carbon mass in the bed was obtained, $m_{ac}^{ad} = 4.8 \times 10^{-3}$ g, corresponding to a surface coverage factor $\sigma = 0.08\%$. This seems to indicate that, once the inert particles' size and mass have been fixed, the adhered activated carbon mass is uniquely determined and is independent of the fluidization velocity.

With the above value of the adhered activated carbon mass, the model was used to calculate the mercury capture efficiency as a function of the free activated carbon mass in the bed for the two fluidization velocities. Results of these calculations are reported in Figs 3 and 4, respectively. In the same figures, horizontal dashed lines corresponding to the experimental mercury capture efficiencies are reported. The model calculations show that at low free carbon loadings, the Hg^0 capture efficiency approaches the value due to the sole contribution of the adhered carbon. When the free carbon mass increases, the Hg^0 capture efficiency increases, slowly approaching 100% capture at high values of m_{ac}^{free} . The intersections between the model curves and the horizontal lines, give an estimate of the free carbon mass establishing at the steady state in the fluidized bed during the experimental runs. It is noted that these values are about 2-3 orders of magnitude lower than the adhered carbon mass. However, the contribution of the free carbon to the mercury capture efficiency is of the same order of that pertaining to the adhered carbon. The reason is obviously that the Hg^0 mass transfer to the activated carbon surface is much more effective for the free particles dispersed in the gas phase.

By comparing results at 0.15 and 0.32 m/s, it is noted that at the higher velocity the free carbon mass necessary to reach a certain Hg^0 removal efficiency

increases by an order of magnitude with respect to the lower velocity. Two reasons cooperate for this result. At the higher velocity the carbon-to-mercury ratio inside the reactor decreases, and the residence time of the free carbon particles in the bed is lower. The estimates of the free carbon loadings indicate that at the higher velocity a higher free carbon mass indeed establishes in the reactor. The explanation of this result is likely connected to the higher gas flow entering the bubble phase and the reduced interaction of the activated carbon particles with the inert bed solids.

At this point it is possible to estimate the average residence time of the activated particles in the fluidized bed by dividing the total carbon loading in the bed ($m_{ac}^{ad} + m_{ac}^{free}$) by the carbon feed rate to the reactor. For the experiments reported in Fig. 1 this calculation gives an estimate of the average residence time in the range 2-4 s. This residence time is about one order of magnitude larger than the gas residence time in the bed, indicating a significant interaction of the activated carbon particles with the inert bed solids, as expected.

It must be underlined that especially at the lower velocity (0.15 m/s) the model assumption of well mixed gas in the dense phase might not be justified. However, in the light of the descriptive, rather than predictive, nature of the model, it is considered that the loss of accuracy is not so significant to change the substance of the results.

CONCLUSIONS

A steady state 1-D model of mercury capture on activated carbon in a fluidized bed is presented, which considers the presence of both free and adhered carbon in the bed. By comparing model results with Hg^0 capture efficiency results from experiments in a fluidized bed, the free and adhered carbon loadings in the bed and their relative contribution to Hg^0 removal were estimated. It appears that the interplay of phenomena like attachment and detachment of the carbon particles to/from the bed particles as well as mass transfer limitations to the adsorbent determine the overall mercury capture efficiency in the reactor. A detailed comprehension of the fluid-dynamic interactions of the injected activated carbon particles with the fluidized bed would be required to bring the model to a predictive level.

ACKNOWLEDGMENT

The experimental/modeling support of Ms. D. Karatza and Mr. D. Scilla is gratefully acknowledged.

NOTATION

A	cross-sectional area of the bed, m^2
c	gas mercury concentration, kg/m^3
d	particle diameter, m
D_{Hg}	molecular diffusion coefficient of mercury, m^2/s
h	fluidized bed height, m
k_g	boundary layer mass transfer coefficient, m/s

K_{be}	bubble-emulsion phase mass transfer coefficient, s^{-1}
K_{eq}	adsorption equilibrium constant, m^3/kg
m	mass, kg
Q_b	mercury exchange between the dense phase and the bubble phase, kg/s
S	exposed surface, m^2
Sh	particle Sherwood number, -
T	temperature, $^{\circ}C$
U	superficial gas velocity, m/s
U_b	average bubble rise velocity in the bed, m/s
V	volume of one bubble/particle, m^3
z	height from the bed distributor, m

Greek letters

δ	volumetric fraction of bubbles in the bed, -
ε_{mf}	bed voidage at incipient fluidization, -
ρ	density, kg/m^3
σ	surface coverage factor, -
μ	viscosity, kg m/s
ω	local mercury uptake on the adsorbent, -
ω_{max}	maximum mercury uptake capacity on the adsorbent, -

Subscripts or superscripts

0	inlet
ac	activated carbon
ad	adhered carbon
b	bubble phase
d	dense phase
eq	equilibrium
$free$	free carbon
in	inert bed
mf	minimum fluidization
out	outlet

REFERENCES

1. EPA, Mercury study report to congress, Report EPA-452/R-97-003, 1997.
2. Pacyna J.M. and Muench J., *Water, Air & Soil Pollution*, 56, 51, 1991.
3. Brown T.D., Smith D.N., Hargis Jr. R.A. and O'Dowd W.J., *Journal of the Air and Waste Management Association*, 49, 628, 1999.
4. Scala F., *Industrial & Engineering Chemistry Research*, 43, 2575, 2004.
5. Scala F., Chirone R., Lancia A. and Scilla, D., *Proc. of 19th Int. Conf. on Fluidized Bed Combustion*, Vienna, Austria, paper 57, 2006.
6. Chirone R. and Salatino P., *Proc. of the 3rd World Congress on Particle Technology*, Brighton, UK, pp. 3257-3268, 1998.
7. Darton R.C., La Nauze R.D., Davidson J.F. and Harrison D., *Trans IChemE*, 55, 274, 1977.
8. Sit S.P. and Grace J.R., *Chemical Engineering Science*, 36, 327, 1981.
9. Karatza D., Lancia A., Musmarra D. and Pepe F., *Proceedings of the Combustion Institute*, 26, 2439, 1996.